THE JOURNAL OF PHYSICAL CHEMISTRY Letters

pubs.acs.org/JPCL Letter

Cooperative Conical Intersection Dynamics of Two Pyrazine Molecules in an Optical Cavity

Bing Gu* and Shaul Mukamel*

Cite This: J. Phys. Chem. Lett. 2020, 11, 5555−5562 Read Online

ACCESS | Metrics & More | Article Recommendations | Supporting Information

ABSTRACT: Hybrid light−matter states in optical cavities, known as polaritons, offer a novel means of manipulating and controlling photochemical processes. We investigate the cooperative cavity photochemistry of two pyrazine molecules undergoing conical intersection dynamics and interacting with a single cavity photon mode by exact quantum dynamics. When the cavity mode is coupled to the electronic transition between the ground and excited states, we find an enhanced polaritonic splitting and collective dark states. These features dominate the cooperative polariton dynamics and can be observed in the transient absorption spectrum.

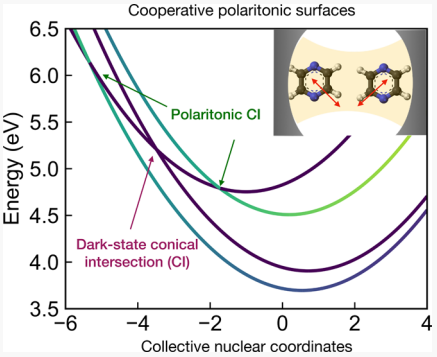

Optical cavities can control electronic and nuclear dynamics[1−19] without chemical modification or external laser pulses. These standing wave cavity resonators of light can be made of, e.g., high-reflectivity mirrors, photonic crystals, and microcircuits.[20] Substantial couplings can be created between electronic transitions of embedded molecules and the confined cavity photon mode even when the cavity is in the vacuum state. The coupling strength $g = \sqrt{N}\boldsymbol{\mu}\cdot\mathbf{e}\sqrt{\frac{\hbar\omega_c}{2\mathcal{V}\epsilon_0}}$, where $\boldsymbol{\mu}$ is the transition dipole moment (TDM), ϵ_0 is the electric permittivity of vacuum, N is the number of molecules in cavity mode volume $\mathcal{V}$, and ω_c and $\mathbf{e}$ are the cavity mode frequency and polarization, respectively. Vacuum fluctuations thus affect the electronic and optical properties of embedded molecules.[21,22] Cavity QED was first discovered by Purcell, who predicted that the spontaneous emission rates of atoms are enhanced when they are placed in a resonant cavity.[23] The strong light−matter coupling regime is realized when g is larger than the loss rate of the cavity mode and the decoherence rate of the molecule. The electronic or vibrational molecular degrees of freedom then combine with the cavity photon to form polaritons. Recent experiments had reported this strong coupling regime[3,20,24] even for a single molecule ($N = 1$) in a cavity vacuum.[6,25−27] The strong coupling has profound effects on photochemical and photophysical processes in molecules, including enhancing the conductivity of organic semiconductors,[28] reversing the selectivity of a ground-state chemical reaction,[29] enhancing the Raman scattering,[6] and enabling long-range energy transfer.[24] These experiments triggered intensive theoretical activity.[1,2,21,30−35]

The bare (no cavity) photodynamics is controlled by the adiabatic Born−Oppenheimer potential energy surfaces (APES), whereas the cavity-controlled photochemistry takes place on the polaritonic potential energy surfaces (PPES) that are modified by the strong light−matter coupling.

Many photochemical reactions occur via conical intersections (CIs) in the APESs. These are molecular geometries in which two APESs are degenerate (intersect) and the electronic and nuclear degrees of freedom become strongly coupled because they evolve on comparable time scales. CIs offer effective channels for electronic excitations to relax nonradiatively to lower electronic states. In the strong coupling regime, the PPESs replace the APESs, and polaritonic CIs then replace the bare CIs. As illustrated in recent theoretical studies,[1,2,5] the PPESs can be very different from the bare APESs and may affect the rates and branching ratios of photochemical processes.[21,36,37]

We have recently found that for a pyrazine molecule that possesses an inherent CI, optical cavities in the strong coupling regime can modify the PPESs by splitting the pristine CI in the APES into a pair of polaritonic CIs in the PPESs,[21] thus influencing the photodynamics. The polaritonic CIs allow a direct relaxation to the electronic ground state from higher-lying excited states. We further showed that cavity control can be robust to environment-induced decoherence, and that the polariton effects on the dynamics may be observed by transient absorption spectroscopy.

Received: February 4, 2020
Accepted: June 12, 2020
Published: June 12, 2020

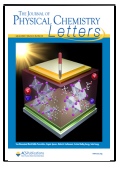

https://dx.doi.org/10.1021/acs.jpclett.0c00381
J. Phys. Chem. Lett. 2020, 11, 5555−5562

While the strong coupling regime has been experimentally realized even for single molecules,[38,39] most polaritonic chemistry experiments rely on many molecules to cooperatively enhance the effective coupling strength through $g \propto \sqrt{N}$.[40] An open issue in cavity photochemistry is whether the $\sqrt{N}$ cooperative enhancement survives decoherence due to coupling to environment and nuclear dynamics, i.e., whether the polaritonic dynamics is dictated by the single-molecule (N = 1) PPES or by the collective polaritonic potential energy surface (CPPES).[37] Another challenge is to identify the spectroscopic signatures of cooperative effects in the polariton dynamics.

Here we study the cooperativity in the polaritonic CIs and its spectroscopic signatures in the pump−probe transient absorption spectrum. We do so by simulating the real-time quantum dynamics of two pyrazine molecules interacting with a single optical cavity mode and compare it with the single-molecule polariton dynamics. Cooperative effects of this system have been studied previously for cavity frequency resonant with the S_0−S_2 Franck−Condon (FC) transition[30] whereby the initial excitation process is modified. Here we focus on the regime in which the cavity mode is close to the transition energy at the CI where the polaritonic CI dominates the cavity photodynamics. We furthur show how the pump−probe transient absorption spectrum (TAS) can monitor the cooperative dynamics. We found cooperative effects when the cavity mode couples to the transition between the ground and excited states (S_0−S_1 vertical excitation). The polariton dynamics of a pair of molecules in the same cavity (model A) or in separate cavities (model B) are compared. We further show that the cooperative polariton effects manifest in the transient absorption spectrum as stronger excited-state absorption (ESA) signals corresponding to transitions from the single-excitation manifold to the double-excitation manifold.

Even though the S_1−S_2 transition is dipole forbidden for pyrazine, it is worth considering the case in which the cavity mode is coupled to S_1−S_2 as a model for more general S_2/S_1 CIs (e.g., uracil). We find no cooperativity in this case; i.e., the dynamics is determined by the single-molecule coupling strength.

Atomic units $\hbar = 1$ are used throughout.

We consider two pyrazine molecules each modeled as a three-electronic-state, two-vibrational mode system[41] interacting with a single cavity photon mode and with external laser pulses

$$H = \sum_{i=1,2} H_{\mathrm{M}}^{(i)} + H_{\mathrm{c}} + H_{\mathrm{CM}}^{(i)} + H_{\mathrm{LM}}(t) \tag{1}$$

where $H_{\mathrm{M}}^{(i)}$ is the molecular Hamiltonian for the ith molecule, H_{C} the cavity field Hamiltonian, H_{CM} the molecule−cavity coupling, and $H_{\mathrm{LM}}(t)$ the interaction between the molecules and classical external light pulses that generate a nonlinear optical response. $H_{\mathrm{M}}^{(i)}$ includes three electronic states and two vibrational modes strongly coupled to the electronic motion, and an S_2−S_1 CI provides an ultrafast electronic relaxation channel (see Figure 1b). This model has been previously used to study nonadiabatic and polariton CI dynamics.[21,30] The diabatic molecular Hamiltonian is given by

$$H_{\mathrm{c}} = \sum_{k=0,1,2} h_k |\psi_k\rangle\langle\psi_k| + \lambda Q_{\mathrm{c}} (|\psi_1\rangle\langle\psi_2| + \mathrm{H.c.}) \tag{2}$$

Here $h_0 = \sum_{j=\mathrm{t,c}} \Omega_j \left(b_j^\dagger b_j + \frac{1}{2} \right)$, $h_k = h_0 + E_k + \kappa_k Q_{\mathrm{t}}$ for $k = 1$ and 2, Q_j and Ω_j denote the dimensionless coordinate of the vibrational modes and the frequency, respectively (j = c denotes the coupling mode and j = t the tuning mode corresponding to the modes coupling diagonally and off-diagonally to the electronic motion), described by the boson creation and annihilation operators b_j and $b_j^\dagger$, $\{|\psi_k\rangle\}$ are the diabatic electronic states, E_k is the vertical excitation energy at the FC point for the kth electronic state, κ_k is the intrastate electron−vibrational coupling constants, and λ is the interstate coupling. The parameters of H_{M} are taken from[42] $\hbar\Omega_{\mathrm{c}}$ = 118 meV, $\hbar\Omega_{\mathrm{t}}$ = 74 meV, E_1 = 3.94 eV, E_2 = 4.84 eV, κ_1 = −105 meV, κ_2 = 149 meV, and λ = 0.262 eV. The cavity Hamiltonian is given by $H_{\mathrm{C}} = \omega_{\mathrm{c}} a^\dagger a$, where ω_{c} is the cavity mode frequency and a and $a^\dagger$ are its boson annihilation and creation operators for photons, respectively. The electric dipole cavity−molecule coupling is

$$H_{\mathrm{CM}} = \sum_n \sum_{i<j} g_{ji}(\mathbf{R})[V_{ji}^{(n)} + V_{ij}^{(n)}](a^\dagger + a) \tag{3}$$

where $\mathbf{R}$ denotes nuclear coordinates, $V_{ji}^{(n)} = |\psi_j^{(n)}\rangle\langle\psi_i^{(n)}|$ is the transition (raising and lowering) operator for the nth molecule, and g_{ji} is the coupling strength for the $|\psi_i\rangle \leftrightarrow |\psi_j\rangle$ transition. The Condon approximation in the diabatic basis leads to $g(\mathbf{R}) = g$. The semiclassical light−matter interaction $H_{\mathrm{LM}}(t) = -\boldsymbol{\mu}\cdot\mathbf{E}(t)$ contains the coupling between the molecules and classical light pulses used in optical measurements, in our case, an actinic pulse and a probe pulse in TAS. The dipole operator is the sum of molecular dipoles $\boldsymbol{\mu} = \sum_n \boldsymbol{\mu}^{(n)}$. In eq 3, we have also neglected the dipole self-energy $\varepsilon_{\mathrm{dip}} = \frac{1}{2\epsilon_0 V} |\mathbf{e}\cdot\boldsymbol{\mu}|^2$ (see ref 43 for its relevance in light−matter interaction).

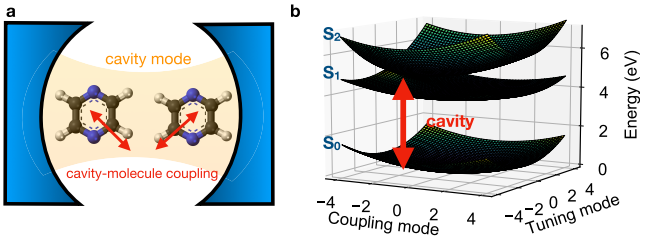

Figure 1. (a) Two pyrazine molecules interacting with a confined cavity photon mode. (b) Aiabatic potential energy surfaces (APES) of pyrazine and the cavity transition frequency considered in this work. Contour maps of the APESs are shown in Figure S1.

Cooperative effects are revealed by comparing the dynamics of models A and B. Because the two molecules are not coupled through the cavity, model B shows the single-molecule polariton dynamics.

The exact nonadiabatic dynamics in the full polaritonic space was solved numerically by expanding the photon−vibronic wave function in a complete basis set: the direct product of the electronic space, vibrational space for the two coupling and two tuning modes, and the cavity photon space. For a single molecule, the polaritonic basis set is a tensor product of the diabatic electronic states $|\psi_k\rangle$, the number of states of the cavity photon mode $|n_{\mathrm{cav}}\rangle$, the number of states of the coupling vibrational mode $|n_{\mathrm{c}}\rangle$, and the tuning vibrational mode $|n_{\mathrm{t}}\rangle$, i.e., $|k n_{\mathrm{cav}} n_{\mathrm{c}} n_{\mathrm{t}}\rangle = |\psi_k\rangle \otimes |n_{\mathrm{cav}}\rangle \otimes |n_{\mathrm{c}}\rangle \otimes |n_{\mathrm{t}}\rangle$. A complete basis for the two-molecule plus single cavity space is given by a tensor product of the basis in each molecule/cavity sub-Hilbert space

$$|\mathbf{k}\mathbf{n}_{\mathrm{c}}\mathbf{n}_{\mathrm{t}}\mathbf{n}_{\mathrm{cav}}\rangle = \left(\bigotimes_{i=1}^{2} |\psi_k^{(i)}\rangle \otimes |n_{\mathrm{c}}^{(i)}\rangle \otimes |n_{\mathrm{t}}^{(i)}\rangle \right) \otimes |n\rangle_{\mathrm{cav}} \tag{4}$$

https://dx.doi.org/10.1021/acs.jpclett.0c00381
J. Phys. Chem. Lett. 2020, 11, 5555−5562

The matrix elements of H_M in this basis are given in the Supporting Information. The resulting basis set size required for the polariton dynamics and TAS simulations is $\sim 4 \times 10^6$. The TAS simulations required a larger basis set than the polariton dynamics because the probe laser pulse can excite the system to the higher-lying states through ESA.

We assume that the two molecules are oriented in parallel (see Figure 1a) and the cavity mode is coupled to the $|\psi_0^{(n)}\rangle \leftrightarrow |\psi_1^{(n)}\rangle$ transition. We start with an impulse optical excitation that brings the molecule into the superposition state

$$|\Psi(0)\rangle = \frac{1}{\sqrt{2}}(|\psi_2^{(1)}\rangle|\chi_0^{(1)}\rangle|\psi_0^{(2)}\rangle|\chi_0^{(2)}\rangle + |\psi_0^{(1)}\rangle|\chi_0^{(1)}\rangle|\psi_2^{(2)}\rangle|\chi_0^{(2)}\rangle)|0\rangle_{cav} \quad (5)$$

where $|\chi_0^{(n)}\rangle$ is the vibrational ground state for the nth molecule.

We describe the cooperative dynamics using the CPPESs. We consider the two molecules as a supermolecule with 3^2 electronic states and 2^2 vibrational degrees of freedom. The electronic states are then given by a tensor product of the individual molecular electronic states $|ij\rangle \equiv |\psi_i^{(1)}\rangle|\psi_j^{(2)}\rangle$. Diagonalizing the polaritonic Hamiltonian $H_p(\mathbf{R}) = H_M + H_C + H_{CM}(\mathbf{R}) - \sum_\alpha T_n^{(n)}$ leads to the cooperative polaritonic states that depend parametrically on nuclear geometry $\mathbf{R}$

$$H_p(\mathbf{R})|\Phi_n(\mathbf{R})\rangle = E_n(\mathbf{R})|\Phi_n(\mathbf{R})\rangle \quad (6)$$

where $E_n(\mathbf{R})$ is the nth CPPES and $|\Phi_n(\mathbf{R})\rangle$ the collective polaritonic states expanded in the electron−photon basis $\{|ij\rangle \otimes |n_{cav}\rangle\}$.

We take the cavity frequency ω_c to be 4.3 eV, close to the electronic transition at the CI. If the cavity frequency is close to the FC transition, the initial state (eq 5) will be modified by polariton effects.[30] The population dynamics of the S_1 state $P_1(t) = \langle\Psi(t)|\sum_n|\psi_1^{(n)}\rangle\langle\psi_1^{(n)}||\Psi(t)\rangle$ for models A and B at $g_{01} = 2000$ cm^{-1} are compared in Figure 2a. Here, $|\Psi(t)\rangle$ is the wave function of the entire polaritonic system. The population dynamics for model A (red line) is very different from that for model B (yellow line) and shows a faster electronic relaxation, implying notable cooperative effects. These effects are also seen in the dynamics of the cavity photon number (Figure 2b). For model B, the photon number is the sum of both cavities. The cavity photon number for model A is smaller than that for model B.

These observations can be understood using the CPPES. A slice of the single-molecule PPES along the tuning mode Q_t is shown in Figure 2c. The strong coupling leads to two polaritonic CIs in the PPESs. The polaritonic nature of the states is encoded in the line color of the surfaces. The CPPES cut along the symmetric tuning mode $Q_t^{(1)} = Q_t^{(2)}$ is shown in Figure 2d. The CPPES can be understood as follows. Assume that the two molecules are in the same nuclear configuration. The single-excitation electronic subspace contains states $\{|S_1S_0\rangle, |S_0S_1\rangle\}$. Because these states are degenerate, any linear combination is also an eigenstate. We choose an equal mixture leading to one bright $|X_{1+}\rangle$ and one dark $|X_{1-}\rangle$ collective exciton state, $|X_{1\pm}\rangle = \frac{1}{\sqrt{2}}(|S_1S_0\rangle \pm |S_0S_1\rangle)$. The collective exciton states $|X_{2\pm}\rangle$ are defined like $|X_{1\pm}\rangle$. Excitons $|X_{j-}\rangle$ are dark because $\langle G|\mu|X_{j-}\rangle = 0$, where $|G\rangle \equiv |S_0S_0\rangle$ is the molecular ground state. The interaction between the ground state and the bright collective exciton is enhanced by a factor of $\sqrt{2}$, i.e.

$$\langle G|\mu|X_{1+}\rangle = \sqrt{2}g \quad (7)$$

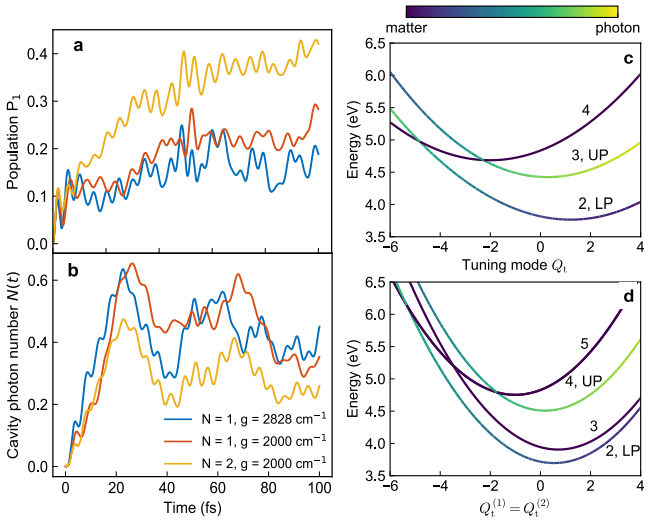

Figure 2. Collective polariton dynamics of two pyrazine molecules strongly coupled to a single cavity photon mode. The cavity mode (ω_{cav} = 4.3 eV) is coupled to the $|\psi_0^{(n)}\rangle \leftrightarrow |\psi_1^{(n)}\rangle$ transition in every molecule. (a) Population dynamics of electronic state S_1 for (yellow) model A and for model B with (brown) the same and (blue) an enhanced coupling strength $\sqrt{2}g_{01}$. For model A, $P_1(t) = \langle\Psi(t)|\sum_n|\psi_1^{(n)}\rangle\langle\psi_1^{(n)}||\Psi(t)\rangle$, where $\Psi(t)$ is the wave function for the full system. (b) Cavity photon number dynamics $N(t) = \langle\Psi(t)|a^\dagger a|\Psi(t)\rangle$. (c) Cut of the polaritonic potential energy surfaces along the tuning mode for a single molecule at g_{01} = 2000 cm^{-1}. (d) Cut of the collective polaritonic potential energy surfaces along the symmetric tuning mode for N = 2. UP and LP denote the upper and lower polaritons, respectively.

This cooperative coupling can be clearly seen in the CPPES cut (Figure 2d), where the Rabi splitting is increased by a factor of ~1.4 compared to the single-molecule PPES (Figure 2c) when molecules share the same geometry. For $N > 2$ molecules, the interaction strength scales as $\sqrt{N}$ along the line where $\mathbf{R}^{(1)} = \mathbf{R}^{(2)} = \cdots \mathbf{R}^{(N)}$.

The cooperative polariton dynamics can be described as follows. The nuclear wavepacket of the supermolecule evolves in the CPPES, whereby avoided crossings and CIs, either intrinsic or light-induced, induce nonadiabatic transitions. Because the cavity resonance is detuned from the excitation energies at the FC geometry, the eigenstates of the full Hamiltonian may still be associated with the bare molecular states in the vicinity of the FC point. An actinic pulse excites the molecules to the bright exciton state $|X_{2+}\rangle$ (labeled state 5 in Figure 2d), whose projection along the two tuning modes is shown in Figure 3. In addition to the bright exciton state, there is a degenerate dark exciton state $|X_{2-}\rangle$. The nuclear wavepacket (projected onto the vibrational subspace of the tuning modes) then moves in the direction of the symmetric tuning mode, following the CPPES slope. When it hits the polaritonic CI, the strong polariton−nuclear coupling induces electronic relaxation to the upper polaritonic surface (labeled 4 in Figure 2d), accompanied by the generation of a cavity photon (Figure 2b).

Another unique feature of the polaritonic surfaces is the presence of collective dark states (CDS), manifested as purely molecular states forming a CI, which has the pristine CI geometry (see Figure 2d). To trace the origin of these CDS, we focus on the single-excitation manifold spanned by the delocaized exciton states $|X_{j\pm}\rangle$, which are all degenerate at the pristine CI. Once coupled to the cavity mode, $|X_{1+}\rangle$ will mix with the cavity photon giving rise to a pair of polariton states. The 3-

https://dx.doi.org/10.1021/acs.jpclett.0c00381
J. Phys. Chem. Lett. 2020, 11, 5555−5562

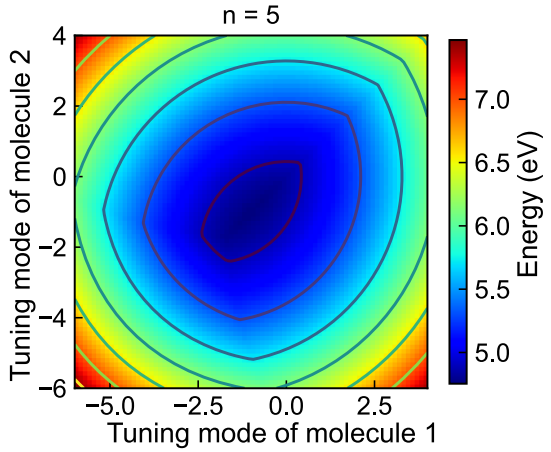

Figure 3. Projection of the fifth collective polaritonic potential energy surface $P_{n=5}$, close to the bright exciton state $|X_{2+}\rangle$ in the Franck–Condon region, which is responsible for the initial wavepacket motion upon photoexcitation.

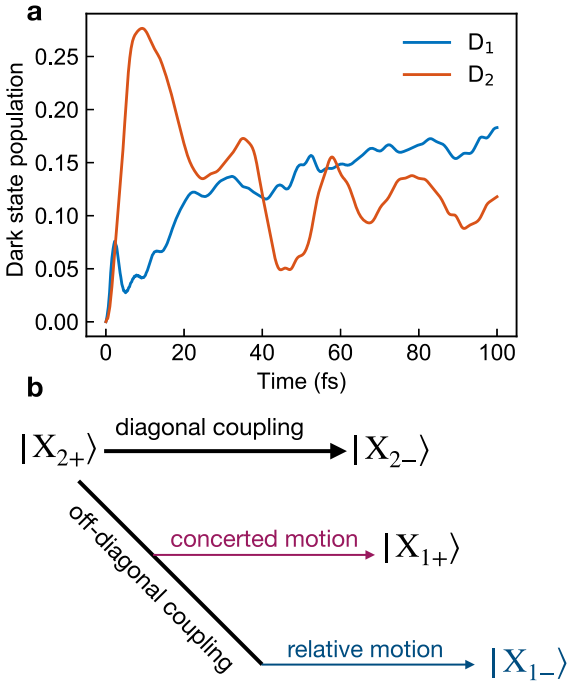

Figure 4. (a) Dark-state population dynamics at $g_{01} = 2000\ \text{cm}^{-1}$ for two pyrazine models interacting with a single cavity photon mode. $D_j(t) = \langle\Psi(t)||X_{j-}\rangle\langle X_{j-}||\Psi(t)\rangle$. (b) Schematic of the vibronic couplings responsible for the dark-state population transfer. The dark states are populated during the population dynamics.

fold degeneracy remains intact for the pair of dark states and the bright exciton state $|X_{2+}\rangle$. When $g_{02} \neq 0$, the degeneracy between the dark excitons $|X_{j-}\rangle$ and $|X_{2+}\rangle$ will be lifted, with the remaining $|X_{1-}\rangle$ and $|X_{2-}\rangle$ forming the CDS-CI. This CDS-CI arises only when the molecules contain pristine CIs in their APESs and is different from the collective CI discussed previously,[37] which requires at least three molecules to emerge. Note that the CDSs are strictly dark only in the subspace where the molecules have the same geometry $\Delta_\sigma \equiv Q_\sigma^{(1)} - Q_\sigma^{(2)} = 0$, where σ labels the vibrational mode. For $\Delta_\sigma \neq 0$, the molecular transition energies are different and one will not find a perfect CDS.

To unveil the role of CDSs in the dynamics, we compare the single-molecule polariton dynamics with an enhanced coupling strength such that the Rabi splitting coincides with the two-molecule case. One would expect the polariton dynamics to be similar irrespective of the number of molecules. However, as shown in panels a and c of Figure 2, this is not the case. This difference is attributed to the CDS. To confirm this, we followed the population dynamics of $|X_{j-}\rangle$, shown in Figure 4a. We find non-negligible population transfer to the CDS during the polariton dynamics. How does the population transfer to CDS occur? CDS may not be directly excited during the initial laser excitation. If nuclear motions are frozen, there is no population transfer to the dark states because the cavity mode influences only the bright states. Population transfer is caused by the electron–vibrational couplings. The vibronic couplings in each molecule can be recast in terms of the collective states (see section S4 of the Supporting Information). The possible coupling schemes are shown in Figure 4b: the diagonal vibronic couplings can induce a transition from the bright exciton $|X_{2+}\rangle$ to the dark exciton $|X_{2-}\rangle$ while the off-diagonal couplings induce transitions to the other manifold of excitons $|X_{1\pm}\rangle$. The concerted motion of both molecules makes a bright–bright transition, and the relative motion causes bright–dark transitions (see Figure 4b). Note that in the adiabatic picture where the polaritonic Hamiltonian depends on the nuclear configuration, the dark states $|X_{j-}\rangle$ are eigenstates of $H(\mathbf{R})$ only in the vicinity of the relative coordinates $\Delta_\sigma = 0$.

The insights gained by comparing the polariton dynamics for $N = 1$ and $N = 2$ can be extended to $N > 2$. Consider N molecules with the same geometry. The polaritonic states can be understood by introducing the collective exciton operators

$$X_{j\alpha}^{\dagger} = \frac{1}{\sqrt{N}} \sum_{n=1}^{N} e^{i2\pi jn/N} |\psi_\alpha^{(n)}\rangle\langle\psi_0^{(n)}| \tag{8}$$

where $j = 0, ..., N-1$. This leads to $N-1$ dark states with $j \neq 0$ and one bright state with $j = 0$ in the single-excitation manifold. The cavity–molecule interaction is then given by $H_{CM} = g_{01}\sqrt{N}(X_{01}^{\dagger} + X_{01})(a + a^{\dagger})$. Thus, the cavity mode interacts with the bright electronic state by an enhanced collective coupling $g_{01}\sqrt{N}$. The Rabi splitting thus scales with $\sqrt{N}$. When nuclear coordinates are taken into account, this collective strong coupling will lead to a pair of polaritonic CIs in the CPPES slice along the line in the configuration space where $\mathbf{R}^{(1)} = \mathbf{R}^{(2)} = ... = \mathbf{R}^{(N)}$. It is then possible to employ the collective strong coupling to manipulate the molecular photochemistry even when the single-molecule coupling is weak provided that the cavity mode is coupled to the transition between the ground and excited states. On the other hand, there are $N-1$ dark exciton states generated by $X_j^{\dagger}, j \neq 0$. The vibronic coupling will induce population transfer from bright polariton states to such dark states.

We now demonstrate how the cooperative effects can be observed by TAS (eq 9). This pump–probe technique provides information about the excited-state population dynamics. The molecule is first excited to an electronically excited state by an ultrashort pump pulse, and afer a variable delay time T, a probe pulse interrogates the molecule and reveals the state-occupation changes

The theory of nonlinear molecular spectroscopy in optical cavities is analogous to that for bare molecules but with the bare molecular states replaced by the hybrid polaritonic states. In

https://dx.doi.org/10.1021/acs.jpclett.0c00381
J. Phys. Chem. Lett. 2020, 11, 5555−5562

TAS, the sample is first excited by a pump pulse, and after a variable time delay T, the sample is interrogated by the probe pulse whereby the changes in the absorbance and/or transmittance are recorded. The transient absorption spectrum is defined as the time-averaged photon flux in the probe pulse, which is given by (see section S2 of the Supporting Information)

$$S_{\mathrm{TAS}}(\omega) = 2\mathrm{Im}[\langle \mathbf{P}(\omega)\rangle \cdot \mathbf{E}_2^*(\omega)] \tag{9}$$

where $\mathbf{E}_2(t)$ $[\mathbf{E}_2^*(t)]$ is the positive (negative) frequency component of the electric field of the probe laser pulse and the polarization $\mathbf{P} \equiv \boldsymbol{\mu}$. In the nonperturbative approach for TAS, we follow the polarization dynamics of the dressed molecules in the presence of both laser pulses. The theory of TAS for polaritons is detailed in the Supporting Information. A perturbative treatment of the laser−matter interaction to the third order leads to several contributions [stimulated emission (SE) and ESA] corresponding to different Liouville space pathways, which can be represented by the time-loop diagrams[44] (see Figure S2). The computational details are given in the Supporting Information.

For a single molecule, the pump pulse brings the molecule into the S_2 surface (Figure 2c). The nuclear wavepacket then propagates down the slope of the surface. The probe pulse at early time delays (T = 5 fs) induces SE from S_2 to S_0, giving rise to the emission band around the FC transition energy S_2−S_0 as shown in Figure 5. We do not observe a large SE signal for $N = 2$ due to the cancellation between ESA and SE at early times. The single molecule does not show ESA at early times due to the vanishing TDM from S_2 to the double-excitation manifold (i.e., $N_X + N_{\mathrm{cav}} = 2$, where $N_X = \sum_n \sum_{k=1,2} |S_k^{(n)}\rangle\langle S_k^{(n)}|$ denotes the number of molecular excitons and N_{cav} the number of cavity photons). The red-shift of the band with the time delay reflects the wavepacket motion on the S_2 surface. Only at $t \sim 20$ fs does the single-molecule nuclear wavepacket reach a polaritonic CI (the one closer to the initial wavepacket) and relax to the upper polariton surface that are superpositions of $|S_0\rangle|1\rangle_{\mathrm{cav}}$ and $|S_1\rangle|0\rangle_{\mathrm{cav}}$. This leads to an increase in the cavity photon number and the ground-state population. The hybrid upper polariton states have nonvanishing TDM to the double-excitation manifold, thus inducing the ESA. For $N = 1$, the double-excitation subspace consists of $|S_1\rangle|1_{\mathrm{cav}}\rangle$, $|S_2\rangle|1_{\mathrm{cav}}\rangle$, and $|S_0\rangle|2\rangle_{\mathrm{cav}}$. Note that in the single-molecule case only polariton states have nonvanishing TDM to the double-excitation states. Pure molecular states cannot be excited to higher-lying polaritons due to the cavity number mismatch. Thus, the ESA can be seen as a unique feature induced by polaritons. There is only an SE signal for the bare nonadiabatic dynamics.[21] For $N = 2$, the double-excitation manifold contains $\{|ij0\rangle \equiv |S_i^{(1)}\rangle|S_j^{(2)}\rangle|n\rangle_{\mathrm{cav}}, |j01\rangle, |0j1\rangle\}, |002\rangle$ for $i, j \in \{1, 2\}$. The ESA can arise from several transitions from the single-polariton surfaces to the double-excitation subspace. The fact that the ESA for $N = 2$ is much stronger than that for $N = 1$ implies that population transfer to the upper polariton surface is faster for $N = 2$, consistent with the polariton dynamics.

Even though the S_1−S_2 transition is dipole forbidden in pyrazine and does not couple to the cavity mode, it is instructive to add such a dipole as a model for more general S_2/S_1 CIs such as uracil.[45] We find no cooperative effects in this case. As shown in Figure 6, the polariton dynamics are identical in models A and B. To rationalize this, we display in panels c and d of Figure 6 the CPPES along the symmetric tuning mode holding the coupling modes fixed at the ground-state equilibrium geometry. The Rabi splitting in the CPPES cut along the $Q_t^{(1)} = Q_t^{(2)}$ now coincides with the single-molecule PPES, in stark contrast to pyrazine

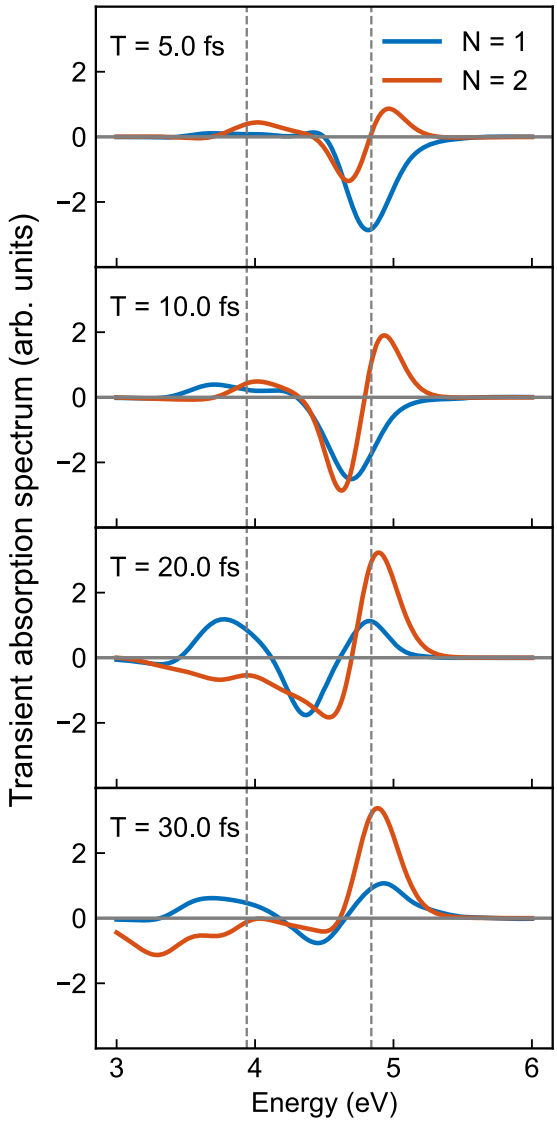

Figure 5. Transient absorption spectrum for $N = 1$ (blue) and $N = 2$ (yellow) pyrazine molecules strongly coupled to a single cavity mode. T is the time delay between the pump and probe pulses, and $g_{01} = 2000$ cm^{-1}. Dashed vertical lines indicate the Franck−Condon transition from the ground state to two excited states in a single molecule. The signal for two molecules interacting with a single cavity mode shows a stronger absorption band around 5 eV due to excited-state absorption.

where the Rabi splitting is enhanced. This can be explained by transforming the single-excitation electronic states into the collective exciton states; the ones that couple to the cavity photon mode are $|X_{j\pm}\rangle, j = 1, 2$. The Rabi splitting is determined by the TDM between $|X_{1\pm}\rangle$ and $|X_{2\pm}\rangle$

$$\langle X_{1\pm}|\mu|X_{2\pm}\rangle = \frac{1}{2}\langle S_2S_0 \pm S_0S_2|\mu|S_1S_0 \pm S_0S_1\rangle = g \tag{10}$$

The Rabi splitting is thus the same as in model B. Equation 10 holds even when the states have permanent dipoles. Here the cavity mode is also coupled to the transition between two dark states $|X_{j-}\rangle, j = 1, 2$, and the polaritonic states are 2-fold degenerate. In contrast to pyrazine where the collective strong coupling dominates the polaritonic dynamics, here it is governed by the single-molecule coupling strength. Thus, manipulating the S_2−S_1 internal conversion process by optical cavities requires strong coupling for a single molecule.

https://dx.doi.org/10.1021/acs.jpclett.0c00381
J. Phys. Chem. Lett. 2020, 11, 5555−5562

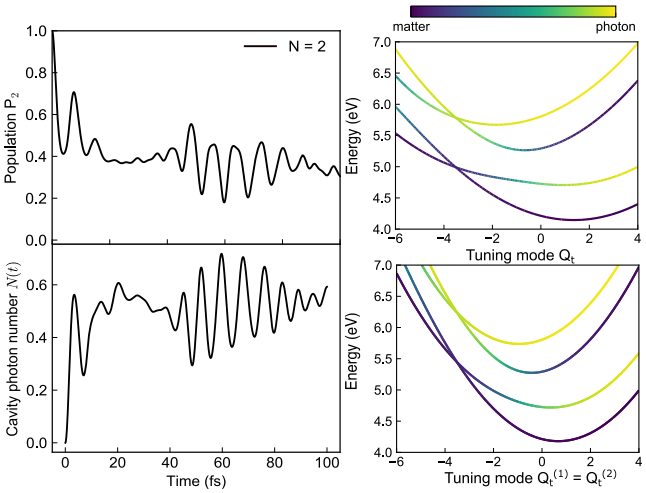

Figure 6. Same as Figure 2 but when the cavity mode is coupled to the $|\psi_1^{(n)}\rangle \leftrightarrow |\psi_2^{(n)}\rangle$ transition in each molecule. Here $\omega_{cav} = 5000\ cm^{-1}$, and $g_{12} = 2000\ cm^{-1}$. The single-molecule polariton dynamics $N = 1$ overlaps with the cooperative dynamics.

This observation may be alternatively understood intuitively without using the collective polariton surfaces. The initial actinic pulse excites one molecule to S_2 while the other remains in the ground electronic state (eq 5). Because the cavity mode couples to only the S_1−S_2 transition, electronic excitations cannot be induced in the unexcited molecule by the cavity photon. Therefore, the molecule in the ground state does not influence the photodynamics of the excited molecule. For cooperative effects to emerge in this case, one has to bring both molecules to the electronic excited state. Even if the S_0−$S_{1/2}$ transitions are included in the molecule−cavity coupling, it requires multiple photons to bring the ground-state molecule to excited states due to frequency mismatch ($E_1/\omega_c \sim 6$). Multiphoton effects may become prominent in the ultrastrong coupling regime where the coupling strength is comparable to the cavity frequency $g \sim \omega_c$.

Our findings also hold for $N > 2$ molecules. To see this, we recast the cavity−molecule coupling (eq 3) in terms of the collective excitons $|X_{j\alpha}\rangle = X_{j\alpha}^{\dagger}|G\rangle$

$$H_{CM} = g_{12} \sum_{j=0}^{N-1} (|X_{j1}\rangle\langle X_{j2}| + \text{H.c.})(a^{\dagger} + a) \tag{11}$$

Equation 11 suggests that increasing the number of molecules when the cavity is coupled to the transition between excited states will not lead to enhanced light−matter coupling but merely increase the degeneracy of the polaritonic states, with the Rabi splitting determined by the single-molecule coupling strength.

In summary, we have investigated the cooperative polariton dynamics for two three-state, two-mode conical intersection models of pyrazine strongly coupled to a cavity photon mode. We find cooperative dynamics of two molecules shows a faster electronic relaxation when the S_0−S_1 transition is coupled to the cavity mode. While the case in which the cavity mode is resonant with the FC transition has been studied recently,[30] here we focus on a cavity detuned from the FC transition and resonant with the electronic transition at the CI point (i.e., the initial excitation remains intact, and the molecule has to undergo a distortion to be resonant with the cavity mode). When the cavity mode couples to a transition between the ground state and an excited state, the CPPESs, and thus the photodynamics, are determined by the collective strong coupling strength, which can be enhanced by increasing the number of active molecules in the cavity mode volume. This suggests that the collective strong coupling can be employed to manipulate photochemical processes (e.g., internal conversion and isomerization) even for a weak single-molecule coupling. We further explored the optical signature of cooperative effects in the pump−probe transient absorption spectrum. The coopeartivity results in a stronger excited-state absorption band compared to the single-molecule polariton dynamics, reflecting the enhanced population transfer due to cooperativity. When the cavity mode couples to the S_0−S_2 transition, the CPPESs contain similar collective features as shown in Figure S3.

We also find no cooperativite polariton dynamics when the cavity mode couples to the $|S_1\rangle$ to $|S_2\rangle$ transition. Manipulating a photochemical process between S_2 and S_1 surfaces requires single-molecule strong coupling. We have analyzed the nature of the polaritonic states and showed that the coupling strength instead of accumulating in the transition between the ground state and the bright delocalized exciton state, is evenly distributed among the transitions between delocalized exciton states and shows no cooperativity.

Whether cooperative effects exist in the polariton dynamics depends on the cavity resonance, cavity−molecule couplings, and initial conditions.[46] Exploring whether cooperative effects can survive the deleterious effects (relaxation and decoherence) of external environments such as photon modes outside of the cavity and solvent is an interesting topic for future studies.

■ ASSOCIATED CONTENT

Supporting Information

The Supporting Information is available free of charge at https://pubs.acs.org/doi/10.1021/acs.jpclett.0c00381.

Matrix elements of the molecular Hamiltonian, theory and computational details for the transient absorption spectrum, and the mechanism for transitions between collective dark states (PDF)

■ AUTHOR INFORMATION

Corresponding Authors

Bing Gu − *Department of Chemistry and Department of Physics and Astronomy, University of California, Irvine, California 92697, United States;* orcid.org/0000-0002-5787-3334; Email: bingg@uci.edu

Shaul Mukamel − *Department of Chemistry and Department of Physics and Astronomy, University of California, Irvine, California 92697, United States;* orcid.org/0000-0002-6015-3135; Email: smukamel@uci.edu

Complete contact information is available at: https://pubs.acs.org/10.1021/acs.jpclett.0c00381

Notes

The authors declare no competing financial interest.

■ ACKNOWLEDGMENTS

The authors thank Dr. Daechum Cho and Dr. Stefano M. Cavaletto for helpful discussions. This work is supported by National Science Foundation Grant CHE-1953045.

REFERENCES

(1) Kowalewski, M.; Bennett, K.; Mukamel, S. Non-Adiabatic Dynamics of Molecules in Optical Cavities. *J. Chem. Phys.* **2016**, *144*, 054309.

(2) Bennett, K.; Kowalewski, M.; Mukamel, S. Nonadiabatic Dynamics May Be Probed through Electronic Coherence in Time-Resolved Photoelectron Spectroscopy. *J. Chem. Theory Comput.* **2016**, *12*, 740−752.

(3) Ebbesen, T. W. Hybrid Light−Matter States in a Molecular and Material Science Perspective. *Acc. Chem. Res.* **2016**, *49*, 2403−2412.

(4) Schäfer, C.; Ruggenthaler, M.; Appel, H.; Rubio, A. Modification of Excitation and Charge Transfer in Cavity Quantum-Electrodynamical Chemistry. *Proc. Natl. Acad. Sci. U. S. A.* **2019**, *116*, 4883−4892.

(5) Galego, J.; Garcia-Vidal, F. J.; Feist, J. Cavity-Induced Modifications of Molecular Structure in the Strong-Coupling Regime. *Phys. Rev. X* **2015**, *5*, 041022.

(6) Shalabney, A.; George, J.; Hiura, H.; Hutchison, J. A.; Genet, C.; Hellwig, P.; Ebbesen, T. W. Enhanced Raman Scattering from Vibro-Polariton Hybrid States. *Angew. Chem., Int. Ed.* **2015**, *54*, 7971−7975.

(7) Flick, J.; Narang, P. Cavity-Correlated Electron-Nuclear Dynamics from First Principles. *Phys. Rev. Lett.* **2018**, *121*, 113002.

(8) Dorfman, K. E.; Mukamel, S. Multidimensional Photon Correlation Spectroscopy of Cavity Polaritons. *Proc. Natl. Acad. Sci. U. S. A.* **2018**, *115*, 1451−1456.

(9) Herrera, F.; Spano, F. C. Cavity-Controlled Chemistry in Molecular Ensembles. *Phys. Rev. Lett.* **2016**, *116*, 238301.

(10) Coles, D. M.; Somaschi, N.; Michetti, P.; Clark, C.; Lagoudakis, P. G.; Savvidis, P. G.; Lidzey, D. G. Polariton-Mediated Energy Transfer between Organic Dyes in a Strongly Coupled Optical Microcavity. *Nat. Mater.* **2014**, *13*, 712−719.

(11) Frisk Kockum, A.; Miranowicz, A.; De Liberato, S.; Savasta, S.; Nori, F. Ultrastrong Coupling between Light and Matter. *Nat. Rev. Phys.* **2019**, *1*, 19−40.

(12) Vasa, P.; Lienau, C. Strong Light−Matter Interaction in Quantum Emitter/Metal Hybrid Nanostructures. *ACS Photonics* **2018**, *5*, 2−23.

(13) Hertzog, M.; Wang, M.; Mony, J.; Börjesson, K. Strong Light−Matter Interactions: A New Direction within Chemistry. *Chem. Soc. Rev.* **2019**, *48*, 937−961.

(14) Hutchison, J. A.; Schwartz, T.; Genet, C.; Devaux, E.; Ebbesen, T. W. Modifying Chemical Landscapes by Coupling to Vacuum Fields. *Angew. Chem., Int. Ed.* **2012**, *51*, 1592−1596.

(15) Flick, J.; Ruggenthaler, M.; Appel, H.; Rubio, A. Atoms and Molecules in Cavities, from Weak to Strong Coupling in Quantum-Electrodynamics (QED) Chemistry. *Proc. Natl. Acad. Sci. U. S. A.* **2017**, *114*, 3026−3034.

(16) Schwartz, T.; Hutchison, J. A.; Léonard, J.; Genet, C.; Haacke, S.; Ebbesen, T. W. Polariton Dynamics under Strong Light−Molecule Coupling. *ChemPhysChem* **2013**, *14*, 125−131.

(17) Herrera, F.; Spano, F. C. Dark Vibronic Polaritons and the Spectroscopy of Organic Microcavities. *Phys. Rev. Lett.* **2017**, *118*, 223601.

(18) Martínez-Martínez, L. A.; Du, M.; Ribeiro, R. F.; Kéna-Cohen, S.; Yuen-Zhou, J. Polariton-Assisted Singlet Fission in Acene Aggregates. *J. Phys. Chem. Lett.* **2018**, *9*, 1951−1957.

(19) Sanvitto, D.; Kéna-Cohen, S. The Road towards Polaritonic Devices. *Nat. Mater.* **2016**, *15*, 1061−1073.

(20) Yang, K. Y.; Oh, D. Y.; Lee, S. H.; Yang, Q.-F.; Yi, X.; Shen, B.; Wang, H.; Vahala, K. Bridging Ultrahigh- Q Devices and Photonic Circuits. *Nat. Photonics* **2018**, *12*, 297−302.

(21) Gu, B.; Mukamel, S. Manipulating Nonadiabatic Conical Intersection Dynamics by Optical Cavities. *Chem. Sci.* **2020**, *11*, 1290−1298.

(22) Bennett, K.; Kowalewski, M.; Mukamel, S. Novel Photochemistry of Molecular Polaritons in Optical Cavities. *Faraday Discuss.* **2016**, *194*, 259−282.

(23) Purcell, E. M. Spontaneous Emission Probabilities at Radio Frequencies. *Phys. Rev.* **1946**, *69*, 681.

(24) Zhong, X.; Chervy, T.; Wang, S.; George, J.; Thomas, A.; Hutchison, J. A.; Devaux, E.; Genet, C.; Ebbesen, T. W. Non-Radiative Energy Transfer Mediated by Hybrid Light-Matter States. *Angew. Chem.* **2016**, *128*, 6310−6314.

(25) Zhong, X.; Chervy, T.; Zhang, L.; Thomas, A.; George, J.; Genet, C.; Hutchison, J. A.; Ebbesen, T. W. Energy Transfer between Spatially Separated Entangled Molecules. *Angew. Chem., Int. Ed.* **2017**, *56*, 9034−9038.

(26) George, J.; Shalabney, A.; Hutchison, J. A.; Genet, C.; Ebbesen, T. W. Liquid-Phase Vibrational Strong Coupling. *J. Phys. Chem. Lett.* **2015**, *6*, 1027−1031.

(27) Benz, F.; Schmidt, M. K.; Dreismann, A.; Chikkaraddy, R.; Zhang, Y.; Demetriadou, A.; Carnegie, C.; Ohadi, H.; de Nijs, B.; Esteban, R.; Aizpurua, J.; Baumberg, J. J. Single-Molecule Optomechanics in "Picocavities. *Science* **2016**, *354*, 726−729.

(28) Orgiu, E.; George, J.; Hutchison, J. A.; Devaux, E.; Dayen, J. F.; Doudin, B.; Stellacci, F.; Genet, C.; Schachenmayer, J.; Genes, C.; Pupillo, G.; Samorì, P.; Ebbesen, T. W. Conductivity in Organic Semiconductors Hybridized with the Vacuum Field. *Nat. Mater.* **2015**, *14*, 1123−1129.

(29) Thomas, A.; Lethuillier-Karl, L.; Nagarajan, K.; Vergauwe, R. M. A.; George, J.; Chervy, T.; Shalabney, A.; Devaux, E.; Genet, C.; Moran, J.; Ebbesen, T. W. Tilting a Ground-State Reactivity Landscape by Vibrational Strong Coupling. *Science* **2019**, *363*, 615−619.

(30) Ulusoy, I. S.; Gomez, J. A.; Vendrell, O. Modifying the Nonradiative Decay Dynamics through Conical Intersections via Collective Coupling to a Cavity Mode. *J. Phys. Chem. A* **2019**, *123*, 8832−8844.

(31) Du, M.; Martínez-Martínez, L. A.; Ribeiro, R. F.; Hu, Z.; Menon, V. M.; Yuen-Zhou, J. Theory for Polariton-Assisted Remote Energy Transfer. *Chem. Sci.* **2018**, *9*, 6659−6669.

(32) Ribeiro, R. F.; Martínez-Martínez, L. A.; Du, M.; Campos-Gonzalez-Angulo, J.; Yuen-Zhou, J. Polariton Chemistry: Controlling Molecular Dynamics with Optical Cavities. *Chem. Sci.* **2018**, *9*, 6325−6339.

(33) Du, M.; Ribeiro, R. F.; Yuen-Zhou, J. Remote Control of Chemistry in Optical Cavities. *Chem.* **2019**, *5*, 1167−1181.

(34) Pérez-Sánchez, J. B.; Yuen-Zhou, J. Polariton Assisted Down-Conversion of Photons via Nonadiabatic Molecular Dynamics: A Molecular Dynamical Casimir Effect. *J. Phys. Chem. Lett.* **2020**, *11*, 152−159.

(35) Zhang, Y.; Nelson, T.; Tretiak, S. Non-Adiabatic Molecular Dynamics of Molecules in the Presence of Strong Light-Matter Interactions. *J. Chem. Phys.* **2019**, *151*, 154109.

(36) Mandal, A.; Huo, P. Investigating New Reactivities Enabled by Polariton Photochemistry. *J. Phys. Chem. Lett.* **2019**, *10*, 5519−5529.

(37) Vendrell, O. Collective Jahn-Teller Interactions through Light-Matter Coupling in a Cavity. *Phys. Rev. Lett.* **2018**, *121*, 253001.

(38) Chikkaraddy, R.; de Nijs, B.; Benz, F.; Barrow, S. J.; Scherman, O. A.; Rosta, E.; Demetriadou, A.; Fox, P.; Hess, O.; Baumberg, J. J. Single-Molecule Strong Coupling at Room Temperature in Plasmonic Nanocavities. *Nature* **2016**, *535*, 127−130.

(39) Wang, D.; Kelkar, H.; Martin-Cano, D.; Rattenbacher, D.; Shkarin, A.; Utikal, T.; Götzinger, S.; Sandoghdar, V. Turning a Molecule into a Coherent Two-Level Quantum System. *Nat. Phys.* **2019**, *15*, 483−489.

(40) Dicke, R. H. Coherence in Spontaneous Radiation Processes. *Phys. Rev.* **1954**, *93*, 99−110.

(41) Woywod, C.; Domcke, W.; Sobolewski, A. L.; Werner, H.-J. Characterization of the S_1−S_2 Conical Intersection in Pyrazine Using *Ab Initio* Multiconfiguration Self-consistent-field and Multireference Configuration-interaction Methods. *J. Chem. Phys.* **1994**, *100*, 1400−1413.

(42) Chen, L.; Gelin, M. F.; Chernyak, V. Y.; Domcke, W.; Zhao, Y. Dissipative Dynamics at Conical Intersections: Simulations with the Hierarchy Equations of Motion Method. *Faraday Discuss.* **2016**, *194*, 61−80.

(43) Rokaj, V.; Welakuh, D. M.; Ruggenthaler, M.; Rubio, A. Light−Matter Interaction in the Long-Wavelength Limit: No Ground-State

https://dx.doi.org/10.1021/acs.jpclett.0c00381
J. Phys. Chem. Lett. 2020, 11, 5555−5562

without Dipole Self-Energy. *J. Phys. B: At., Mol. Opt. Phys.* **2018**, *51*, 034005.
(44) Mukamel, S. *Principles of Nonlinear Optical Spectroscopy*; Oxford University Press, 1995.
(45) Keefer, D.; Thallmair, S.; Matsika, S.; de Vivie-Riedle, R. Controlling Photorelaxation in Uracil with Shaped Laser Pulses: A Theoretical Assessment. *J. Am. Chem. Soc.* **2017**, *139*, 5061−5066.
(46) Vendrell, O. Coherent Dynamics in Cavity Femtochemistry: Application of the Multi-Configuration Time-Dependent Hartree Method. *Chem. Phys.* **2018**, *509*, 55−65.

https://dx.doi.org/10.1021/acs.jpclett.0c00381
J. Phys. Chem. Lett. 2020, 11, 5555−5562